Efficient NVH evaluation of electric motors by means of 2D Fourier analysis on the complex representation of airgap forces

S. Gungl, T. Kimpian
thyssenkrupp Components Technology Hungary Ltd.
Budafoki way 56, 1117 Budapest, Hungary

Abstract
Thanks to the growing popularity of hybrid and fully electric vehicles arose a need for quieter electric motors. Estimating the emitted noise by these motors is a well-established procedure, which uses an electromagnetic and mechanical FEM simulation tool chain. This method requires a lot of calculation especially on the mechanical FEM side. However, meaningful information can be acquired just by analysing the electromagnetic forces. In this paper we propose a way to represent the lumped forces acting inside of the motor during a complete revolution in a complex valued matrix. Calculating the 2D FFT of this matrix yields a 2D spectrum which expresses the temporal and spatial frequencies and their relationship in a single diagram. With this method each harmonic component – unique in time and space – can be analysed individually. Furthermore it is briefly explained how the 2D spectrum can also be filtered and fed into the mechanical FEA, allowing for analysis of the effects of each temporal and spatial harmonic component of the system response.

1 Introduction

Acoustic engineers nowadays face an ever-growing challenge in the automotive industry. Expectations for the acoustic behaviour of the vehicles rise continuously, creating a justified demand for more comfort and better acoustic ergonomics in the newer models. This of course includes generally reducing airborne noise whose characteristics can vary from brand to brand, but also the careful acoustic design of each and every part of the passenger compartment. These acoustic engineering processes are collectively referred to as Noise Vibration and Harshness or NVH for short, which involves the study and adjustment of noise and vibration characteristics in vehicles by means of measurement and simulation. The continuous acoustic development loop caused by the adaptive nature of human hearing is shown on 1. There are generally four main sources of noise in vehicles. Reducing the effect of the loudest source will result in a lower overall noise level, but our hearing quickly adapts and finds the second loudest source disturbing, especially when that is a tonal noise with well-defined frequency components.

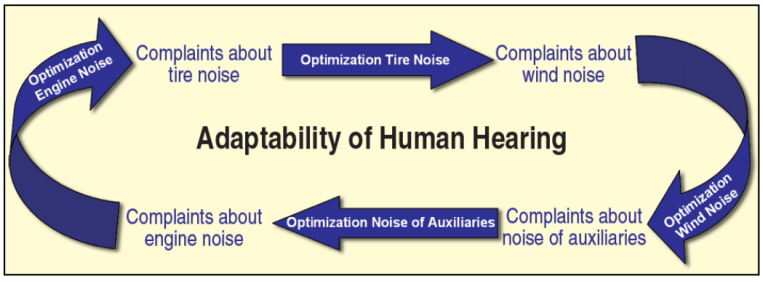

Figure 1: Never-ending development process [1]

Thanks to the growing popularity of electric drivetrains one of the main noise source, the internal combus-

tion engine disappeared from the vehicles and therefore the noise limit for the auxiliary devices – such as the electric power assisted steering systems or EPAS – dropped around 20 dB in an instant. This is because in hybrid, and fully electric vehicles there is virtually no background noise at standstill. The lack of this masking noise makes the previously hidden sounds audible e.g.: sensor, quantization, and controller frequency noise. This will diminish the quality of comfort, and since the drivers are not used to noise of this nature, it might give them a reason to suspect unnatural behaviour, or failures in the system. These grounds motivate vehicle manufacturers to define strict acoustic specifications towards suppliers which in turn will challenge developers to continuously improve their products.

2 Structure of EPAS systems

thyssenkrupp Presta AG (in Hungary known as thyssenkrupp Components Technology Hungary Kft.) has been developing Electric Power Assisted Steering systems for more than two decades. Unlike in the older hydraulic systems, in EPAS – as the name suggests – the assist power is provided by an electromechanical source.

Figure 2: 1.: Steering column, 2.: Intermediate shaft, 3.: Electric power assist

The structure of an electric power assisted steering system is shown on Figure 3. The force exerted on the steering wheel by the driver is measured by the torque sensor unit (TSU) and its data is processed by the electric control unit (ECU). Using this information the controller algorithm calculates the necessary phase currents to create the required assist torque on the shaft of the motor. This torque is then transferred all the way to the wheels through the belt drive (BD), ball nut assembly (BNA) and the steering rack.

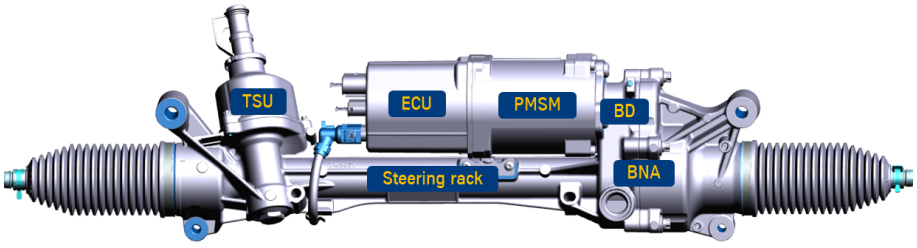

Figure 3: Main parts of the steering rack

The type of systems are called Rack Electric Power Steering (REPS), but there are various different kinds of other steering systems, which are usually categorised by where and how the power assist is applied.

From an acoustics point of view these systems are quite complex and by no means linear and therefore there

are a lot of possible noise inducing mechanisms hidden, but it is generally true the main focus of the acoustic design should be the electric motor and the mechanical transfer path directly connected to it.

3 Electric drivetrains as noise sources

The increasing popularity of partly or fully electric drivetrains and the thriving of the electromagnetically-excited Noise, Vibration, and Harshness scientific field go hand in hand. The focus of eNVH is simulating, modelling, and understanding the noise inducing effects of said drivetrains, with the aim of reducing the noise emission as much as possible. Although this has been a heavily researched topic for a long time [2], new advancements have been made recently, with more and more companies [3] appearing on the market, whose goal is to predict, and in the end lower the noise generated by these systems. Tried and tested simulation softwares are extended with new modules tailored for these sort of analyses and predictions. [4]

3.1 Noise inducing mechanisms of electric motors

The main noise sources of an electric machine are shown on Figure 4. The mechanical and electromagnetic sources can induce dynamic forces, which will then cause vibrations to travel down the mechanical parts of the system, this is called structure-borne noise. The sum of the structure-borne and directly emitted airborne noise will determine the overall noise level of the system. The electromagnetic source will of course be influenced by the harmonic content of the current driving the windings and thus the quality of the motor's control algorithm will also play a vital role in the noise emission of the whole system.

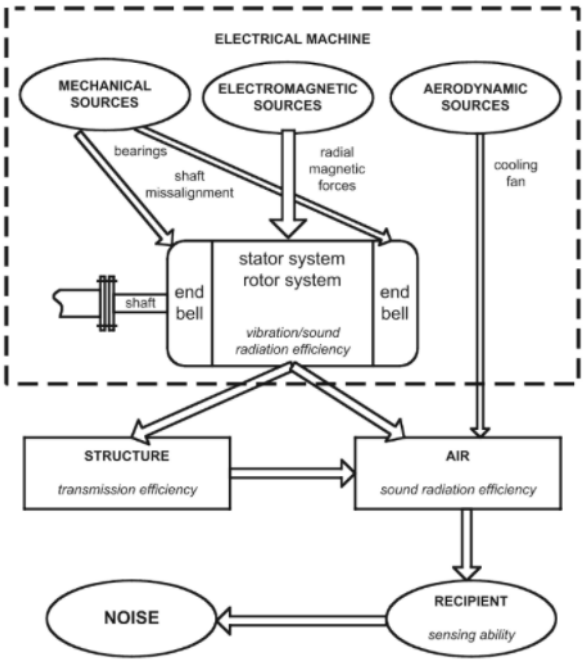

Figure 4: Noise sources of electric motors and possible transfer paths [2]

In EPAS systems the most dominant of the three is the electromagnetic noise source which is always present in the system, regardless of the quality of the manufacturing process. The mechanical sources introduced by the manufacturing imperfections also have to be accounted for – these are most commonly manifested as bearing noise – but with an adequate quality control these do not present an issue in the final system. Considering all of the above, this paper is focusing on the electromagnetic aspects which can be influenced during the design phase of the systems.

3.2 Electromagnetic noise source in PMSM

The noise generation mechanism of permanent-magnet synchronous motors (PMSM) can be seen on Figure 5. In the first stage (1) a 3-phase PWM controlled H-bridge creates the necessary voltages for the stator so that the required torque calculated by the controller can be achieved. This voltage will drive a current in the stator which is dependent on the motor parameters: resistance, inductance, counter-electromotive force. The current will produce a magnetic field, which interacts with the permanent magnets and creates a force distribution on the stator teeth (2). These forces are a function of the rotor position and have a fundamental frequency equal to the shaft frequency, and can be used as the excitation for the mechanical models of both the stator and rotor to calculate the mechanical vibrations of the system (3). Finally using the vibration values the acoustic emission can be calculated (4).

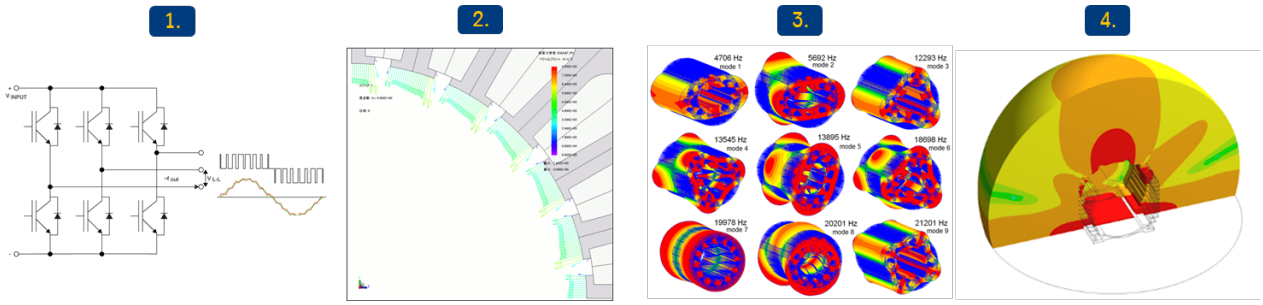

Figure 5: Noise generation in electric motors [5] [6] [7] [8]

3.3 Electromagnetic force calculation methods

There are several different methods for calculating the dynamic forces present in electric motors, out of which the two most commonly used are the Virtual Work Principle (VWP) and the Maxwell Stress Tensor (MST). The question of which approach is more suitable to calculate the forces is a heavily researched topic [9]. From time to time a new and novel approach appears [10], but the most widely used methods in commercial finite element simulation (FEM) softwares are the MST based techniques, which are favourable for lower computation work. As can be seen on Figure 5 using the calculated forces as the excitation for the mechanical FEM the model response can be calculated. This response can arbitrarily be either the vibration at any point on the motor, or the transferred force at the connection interface points. The latter can be further used as the mechanical excitation of the whole steering system. It is worthwhile to examine in detail the forces acting solely on the stator, since for each motor type – in EPAS systems typically a fractional-slot PMSM – the forces have unique characteristics, and recognizing these patterns can help understanding the nature of the noise generated by the motors. In order to do this, we first replace the continuous force distribution acting on the surface of each tooth with a net force and torque pair as it can be seen on Figure 6. This substitution will greatly simplify the projection between different FEM mesh grids, for example the electromagnetic FEM mesh is much finer on the tooth tip than the mechanical mesh. Furthermore it also makes it easier to analyse the temporal and spatial dependency of the forces. The result of this transformation is often called lumped force representation.

4 Complex force representation

The simulated operation of the motor can be represented by a complex valued matrix, which is arbitrarily constructed so that each column represents the force evolution for each tooth as a function of the rotational angle. In other words, each row represents the forces at a given time instant as a function of the spatial position — i.e., for each tooth. This is a convenient representation since it encloses both the time and space dependent behaviour. To be precise we ought to talk about angular values instead of time instants since

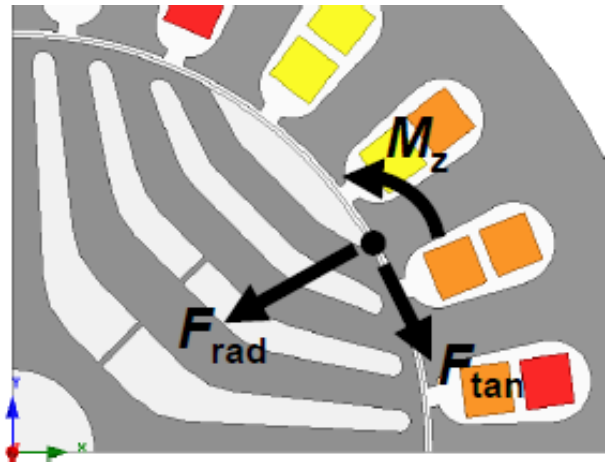

Figure 6: Lumped force representation of the continuous force distribution [11]

the electromagnetic simulations are performed for each angle position of the rotor, but we will keep using temporal and spatial dependencies to avoid ambiguities.

$$F(\theta) = \begin{bmatrix} f_1(\theta_1) & f_2(\theta_1) & \dots & f_M(\theta_1) \\ f_1(\theta_2) & f_2(\theta_2) & \dots & f_M(\theta_2) \\ \vdots & \vdots & \ddots & \vdots \\ f_1(\theta_N) & f_2(\theta_N) & \dots & f_M(\theta_N) \end{bmatrix} \tag{1}$$

It is important to note that the force matrix can be considered a complex (or $\mathbb{R}^2 \to \mathbb{C}$) function since the input space is two-dimensional (time and space dependency) and the output space is the complex plane (force vectors simulated in a 2D environment).

4.1 Temporal harmonics

Time dependent behaviour of the forces can be analysed by taking the FFT of each column of the force matrix, which will yield a traditional 1D spectrum. If the input data is truly complex, meaning it has real and imaginary components, then the spectrum will be asymmetric.

$$Ae^{j\omega t} + Be^{-j\omega t} = (A+B)\cos(\omega t) + i(A-B)\sin(\omega t) \tag{2}$$

First, if we only look at the amplitude spectrum — ignoring the phase — then it can be easily shown (2), that the size of the real and imaginary components will be determined by the sum and difference of the peak amplitudes accordingly. These values also align with the major and minor axes of the ellipse traced out by the given complex harmonic as we can see it on Figure 7.

If the amplitudes of the two peaks are equal and so are the phases, then we get back the traditional symmetric spectrum and the corresponding real valued function. The phases of the peaks will determine the rotation around the origin of the shape described in (2). For example the force function of two peaks with equal amplitudes and phases $\phi_1 = 0, \phi_2 = \pi/6$ can be seen on Figure 7.

The resulting force function will have one degree of freedom since the behaviour of the force vector can be described with only a scalar, despite the fact that it has real and imaginary components. We can highlight two special cases: first when the peaks are complex conjugate pairs (the complex values are symmetric to the x axis) the resulting force force function will be real valued; second if the peaks are symmetric to the y axis, then the resulting force will be purely imaginary.

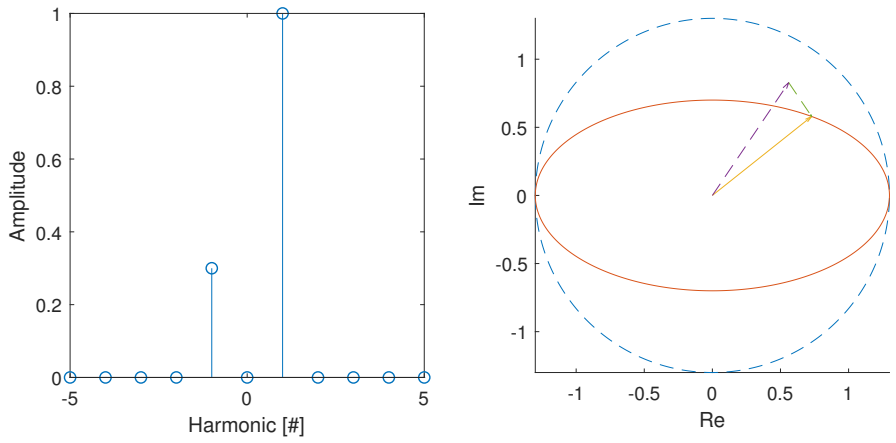

Figure 7: Asymmetric spectrum (left) and corresponding complex force function (right)

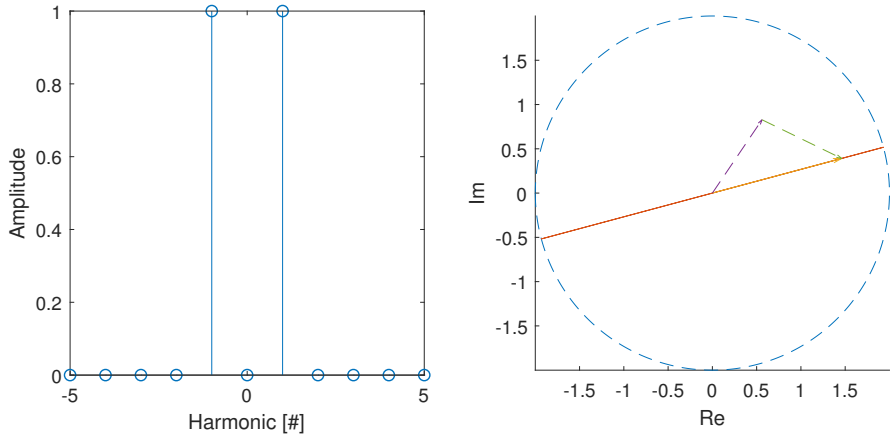

Figure 8: Symmetric amplitude spectrum with phases $\phi_1 = 0, \phi_2 = \pi/6$ (left) and corresponding complex force function (right)

This distinction comes in handy when one wants to separate the force vectors into radial and tangential components acting on each tooth. If we consider each force in their respective local coordinate systems, then the real and imaginary parts will represent the radial and tangential components of the forces respectively.

4.2 Spatial harmonics

The spatial behaviour of the forces can be analysed by applying FFT to each row of the force matrix (1). The meaning of this space-dependent spectrum can be interpreted with the help of Figure 9. Each harmonic component is ”wrapped around” the stator and the resulting shape will indicate the deformation pattern that the motor suffers during its operation. These force patterns correlate well with the mode shapes found in the classic mechanical modal analysis.

This wrapping of the base functions is, in essence, a transformation between local and global coordinate systems. It can be achieved with multiplying each column in the force matrix by a complex vector (Figure 10). If FFT was applied without rotating the vectors first, then each spatial harmonic would get shifted by one. This is because an extra rotation is counted, while going around the circumference of the motor. This effect is also known as the ”coin paradox”.

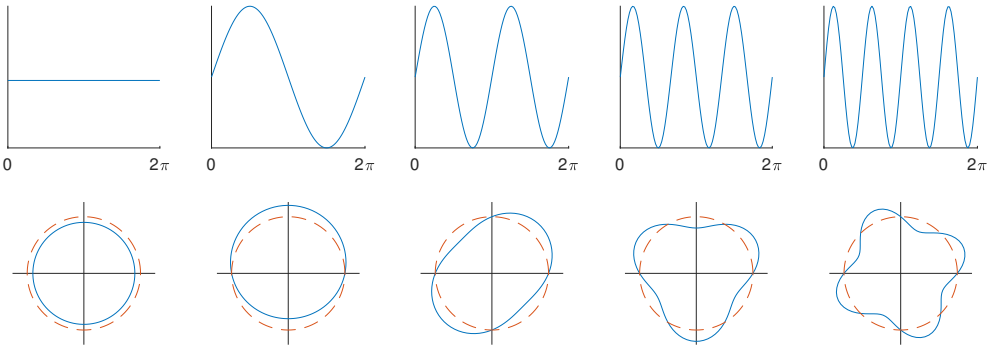

Figure 9: Spatial basis functions

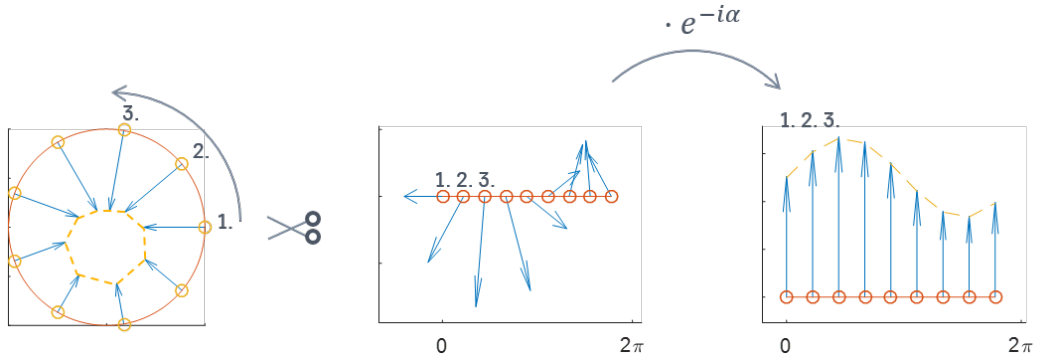

Figure 10: ”Unrolling” the stator

4.3 2D FFT

A two-dimensional Fourier transform can be calculated by applying FFT to the columns and rows (time and space axes) of the force matrix. This 2D spectrum of the complex force matrix is a holistic representation of temporal and spatial harmonics at the same time. The horizontal axis represents spatial, the vertical axis represents temporal harmonics (orders).

Basis functions of the 2D FFT are the same as in 1D — a set of $e^{j\omega t}$ rotating vectors — but the resulting force image is a bit more complex. The basis vectors can rotate as a function of time, and also as a function of spatial position. This effect is shown on Figure 11. As we can see, both peaks are at the first temporal order which means, individual vectors will rotate counter-clockwise. On the other hand they are positioned at the positive and negative 3$^{\text{rd}}$ order. We can see the effects of the latter on the diagram: as we go around the circle counter-clockwise, the vectors turn in different directions based on the sign of the temporal order.

These single peaks hardly show up in actual simulations, however similarly to how a pair of peaks can create a real valued signal in a traditional FFT, here a pair of point symmetric peaks can create attainable force patterns. In Figure 12. we can see how the sum of the two basis functions can create purely radial and tangential forces. Similarly to what we have shown on Figure 8., if the peaks are complex conjugate pairs, forces are radial, if they are symmetric to the imaginary axis (the real part is multiplied by minus one) then the forces are tangential.

One additional dimension is not displayed on these diagrams, and that is time dependency. The sum of two point symmetric peaks will be a travelling wave, rotating around the circumference of the motor, which is analogous with rotating mode shapes. The movement speed and direction will be determined by the angle of the line connecting the peaks. If the peaks were in the 2$^{\text{nd}}$ and 4$^{\text{th}}$ quadrant then the wave would travel in the

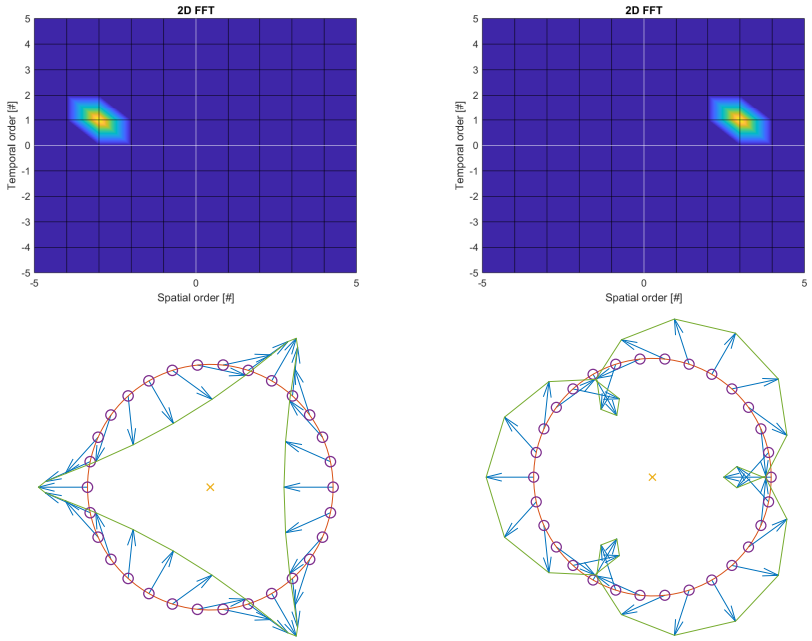

Figure 11: 2D FFT basis functions

opposite direction. The sum of two waves, travelling in the opposite directions is a standing wave with the same shapes as the two travelling waves.

If we take the resulting surface from the 2D FFT and look at it from one of its sides — looking at either the x-z or y-z plane — then we can see the amplitude (z axis) of the spatial or temporal orders. Of course the orders are stacked behind one another, but by calculating the average for example, they can be displayed on a one-dimensional diagram. This is illustrated on Figure 13. In this paper we use the force distribution of a 12 slot, 8 pole motor as an example.

Spatial orders show how the force distribution on the stator is trying to deform the motor, i.e. what regular polygonal shape it is trying to deform it to, while the temporal harmonics tell us how many times the force vector on a single tooth oscillates during one revolution. For example if we look at 4^{th} spatial and 8^{th} temporal harmonic then what we see is a square deformation shape which will rotate around twice — each of the 4 corners passes every tooth twice.

By filtering this complex force matrix — either in the frequency or spatial-temporal domain — we can display the behaviour of each individual harmonic. In the top row of Figure 14 we can see the filtered two-dimensional Fourier transform of the complex force matrix, and in the bottom row the lumped forces at a given rotor position (time instant).

A case of constant motor torque is shown on Figure 14 (a). This DC torque corresponds to 0th temporal and spatial order, since it is a constant value in time and also for each tooth as well. It is interesting to see that the radial component of the lumped forces is much larger compared to the tangential component which is responsible for creating the valuable net torque of the motor.

The second largest spectral force component is the spatial 4^{th} and temporal 8^{th} harmonic, which is trying to deform the motor to a square (or a 4 pointed star). The amplitude of this dynamic force is comparable to the static radial force of the DC torque. This observation is backed up real life measurement data of motors and complete systems as well, where the most dominant harmonic of a 12/8 motor is the 8^{th} order.

With this method we can individually analyse each and every order and oftentimes without even running the full mechanical FEM we can determine the main problem sources from an acoustic point of view. Another interesting and practically important combination of orders, 24th temporal and 0th spatial is shown on Figure 14. (c). In this particular case the phase and direction of each lumped force vector is the same and therefore

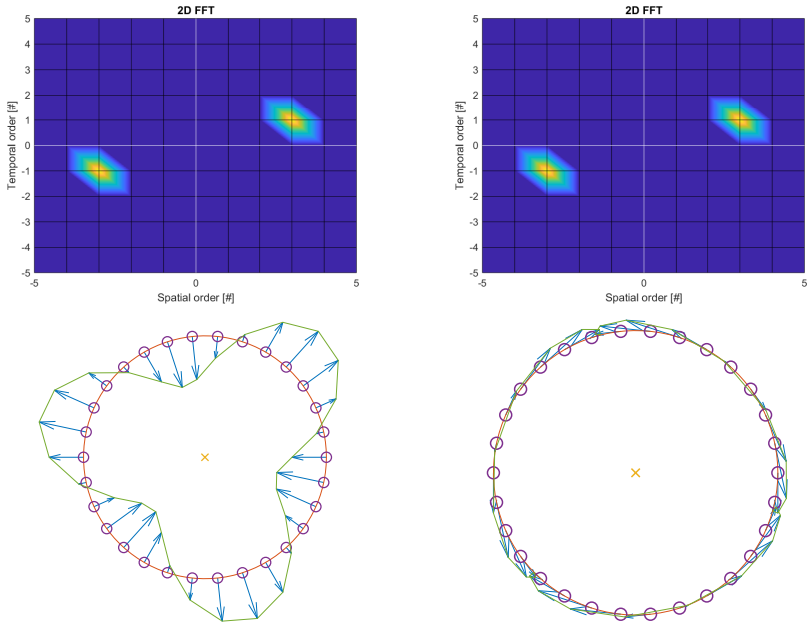

Figure 12: 2D FFT peak pairs with different phases

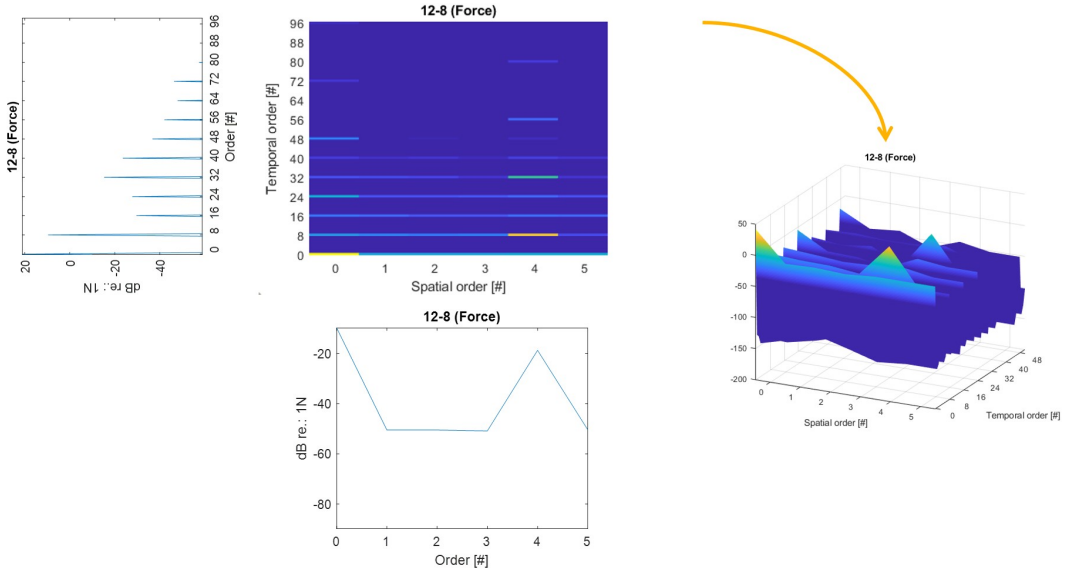

Figure 13: Temporal and spatial orders are two different projections of the 2D complex force spectrum

this will not only deform the stator but it will create a measurable torque ripple on the rotor as well. Although the amplitude of these forces is much smaller than the 8th order, if we analyse the acoustic performance in vehicles the 24th vibration and noise harmonic is still dominant, which means that any harmonic content in the motor torque will most likely transform into disturbing audible noise. These examples should convey the importance of understanding the force development inside of electric motors when it comes to overcoming acoustic problems in manufacturing processes and final products.

Interpreting the results of a 2D FFT can be a challenging task even for someone who is intimately familiar with various force patterns. In order to make the diagrams more intuitive and descriptive we propose a new way of displaying the 2D FFT. Taking advantage of the fact that pairs of peaks construct the force pattern, we can flip and add the negative temporal frequencies to calculate the ratio of radial and tangential force

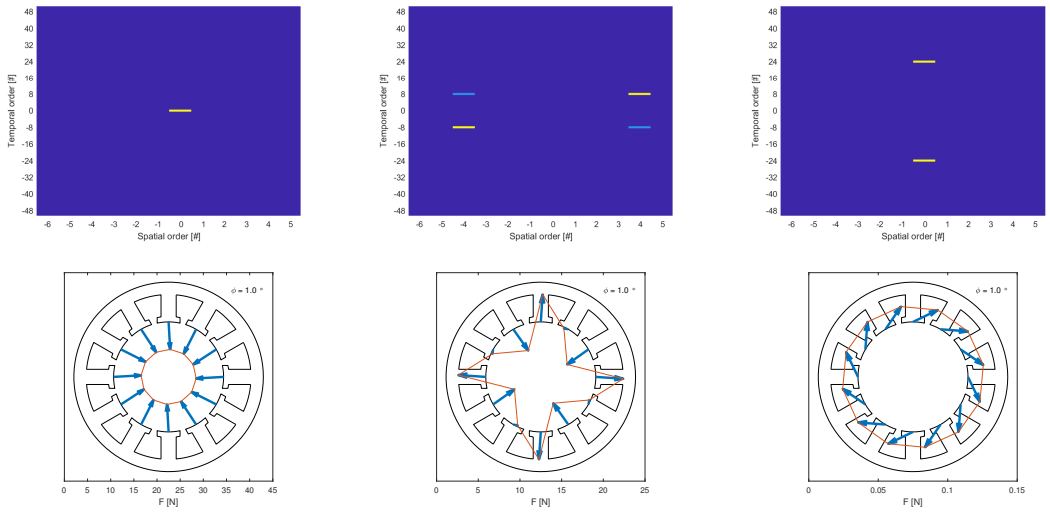

(a) DC (b) 4th spatial 8th temporal (c) 0th spatial 24th temporal

Figure 14: Filtered force matrices in spectral and space-time domain

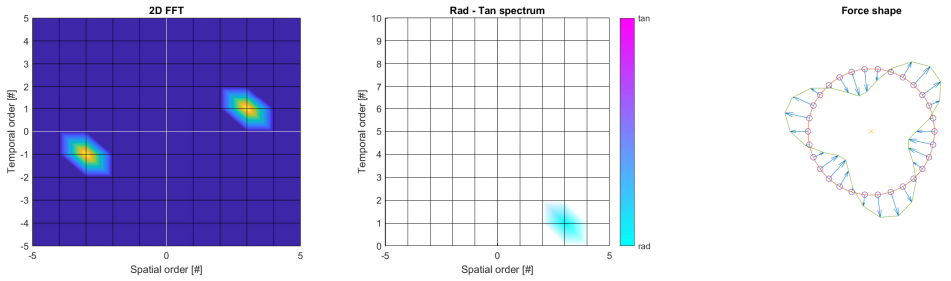

Figure 15: Temporal and spatial orders are two different projections of the 2D complex force spectrum

components. The intensity of the resulting colour scale can then be scaled by the amplitude to only show dominant harmonics. This radial-tangential spectrum is shown on Figure 15

4.4 Calculating mechanical vibrations

Mechanical vibrations of a motor or a whole system can be efficiently calculated using modal decomposition. The first step is to identify the natural frequencies (eigenfrequencies) and modal shapes of the model and then apply the previously discussed lumped forces as excitation. The response noise or vibration of the system can be calculated by utilising modal superposition. One great advantage of this approach is that the input forces can be filtered and pre-processed arbitrarily, so the effects of the various excitations can be separated and analysed individually.

Similarly to studying the forces, it can be helpful to find general patterns and behaviours to better understand the acoustic nature of these complex systems. Figure 16 shows the vibration shapes of a long and thin cylinder.

In the typical operating range the acoustic characteristics of a motor are determined by the 2nd, 3rd, 4th, etc. circumferential, and the 1st longitudinal modes. This is because in an assembled motor the two shields at the either end of the cylindrical body create a rigid connection and so the displacement at the ends is practically zero.

It is worth noting that the circumferential modes have the exact same shapes as the lumped force harmonics

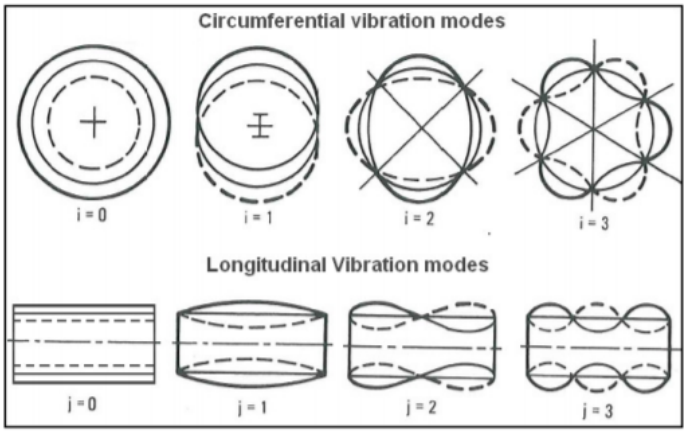

Figure 16: Vibration modes of a finite long, thin cylinder [12]

of the 2D Fourier transform, and therefore it can be easily determined which excitation component of a given motor design will be amplified by the natural frequencies of the mechanical structure. In other words, we can see which modal shapes – with a given eigenfrequency, and modal stiffness – will constitute to the final vibration excited by a certain force harmonic. This information can be valuable for motor engineers and it can aid the development of the systems by taking acoustics aspects into account already at the design phase.

5 Conclusion

In this paper we briefly introduced the acoustic or NVH topics currently researched in the automotive industry and highlighted how the increasing popularity of the electric drivetrains influence the rising acoustic expectations of the auxiliary systems, such as the electric power assisted steering. We described the noise generating mechanisms of the widely used permanent magnet synchronous motors and showed a couple conventional techniques of how these systems could be analysed. We also introduced a new way of separating and analysing the excitations and their effects in the final product.

Acknowledgements

The authors would like to express their gratitude to thyssenkrupp Components Technology Hungary for making this research project possible and to all the exceptional colleagues who provided insight and expertise.

References

[1] K. Genuit, “Vehicle interior noise - a combination of sound, vibration and interactivity,” in *INTER-NOISE and NOISE-CON Congress and Conference Proceedings*, vol. 2, 01 2008, pp. 1025–1035.

[2] J. Gieras, C. Wang, and J. Lai, *Noise of Polyphase Electric Motors*, 01 2005.

[3] K. Degrendele, M. Glesser, and J. LE BESNERAIS, “Mécanismes de génération du bruit et des vibrations d’origine électromagnétique dans les moteurs électriques,” 03 2020.

[4] ANSYS, “Electric motor design, analysis and verification,” https://www.ansys.com/applications/electric-motors.

[5] infineon, “Electronics 101,” http://www.irf.com/electronics/topology-fundamentals, accessed: 2022-05-20.

[6] JMAG, "Starting with vibration noise analyses vol. 1 (motor edition 1)," https://www.jmag-international.com/motor_design_develop/motor_01/, 2014, accessed: 2022-05-20.

[7] M. A. H. Rasid, "Contribution to multi-physical studies of small synchronous-reluctance machine for automotive equipment," Ph.D. dissertation, 02 2016.

[8] CADFEM, "Electric drive acoustics inside analysis," https://www.cadfem.net/en/our-solutions/cadfem-ansys-extensions/electric-drive-acoustics-inside-ansys.html, 2015, accessed: 2021-09-04.

[9] R. Pile, E. Devillers, and J. LE BESNERAIS, "Comparison of main magnetic force computation methods for noise and vibration assessment in electrical machines," *IEEE Transactions on Magnetics*, vol. 54, pp. 1–13, 05 2018.

[10] D.-H. Kim, D. Lowther, and J. Sykulski, "Efficient force calculations based on continuum sensitivity analysis," *Magnetics, IEEE Transactions on*, vol. 41, pp. 1404 – 1407, 06 2005.

[11] Wibbeler, J., "Noise generated by electric drives," CADFEM Webinar, 2020.

[12] Z. E. Khawly and D. Schramm, "Analytical modal analysis for the stator system of a permanent magnet synchronous motor for hybrid vehicles and calculation of its natural frequencies," in *Proceedings of ISMA2010 including USD2010*, Leuven, Belgium, 2010, pp. 4535–4548.